Relation Between Coronary Plaque Composition Assessed by Intravascular Ultrasound Virtual Histology and Myocardial Ischemia Assessed by Quantitative Flow Ratio

Jeff M. Smit, MD[a], Mohammed El Mahdiui, MD[a], Michiel A. de Graaf, MD, PhD[a], José M. Montero-Cabezas, MD[a], Johan H.C. Reiber, PhD[b,c], J. Wouter Jukema, MD, PhD[a], Arthur J. Scholte, MD, PhD[a], Juhani Knuuti, MD, PhD[d], William Wijns, MD, PhD[e], Jagat Narula, MD, PhD[f], and Jeroen J. Bax, MD, PhD[a,d,*]

Coronary plaque composition may play an important role in the induction of myocardial ischemia. Our objective was to further clarify the relation between coronary plaque composition and myocardial ischemia in patients with chest pain symptoms. The study population consisted of 103 patients who presented to the outpatient clinic or emergency department with chest pain symptoms and were referred for diagnostic invasive coronary angiography. Intravascular ultrasound virtual histology was used for the assessment of coronary plaque composition. A noncalcified plaque was defined as a combination of necrotic core and fibrofatty tissue. Quantitative flow ratio (QFR), which is a coronary angiography-based technique used to calculate fractional flow reserve without the need for hyperemia induction or for a pressure wire, was used as the reference standard for the evaluation of myocardial ischemia. Coronary artery plaques with QFR of ≤0.80 were considered abnormal—that is, ischemia-generating. In total, 149 coronary plaques were analyzed, 21 of which (14%) were considered abnormal according to QFR. The percentage of noncalcified tissue was significantly higher in plaques with abnormal QFR (38.2 ± 6.5% vs 33.1 ± 9.0%, p = 0.014). After univariable analysis, both plaque load (odds ratio [OR] per 1% increase 1.081, p <0.001) and the percentage of noncalcified tissue (OR per 1% increase 1.070, p = 0.020) were significantly associated with reduced QFR. However, after multivariable analysis, only plaque load remained significantly associated with abnormal QFR (OR per 1% increase 1.072, p <0.001). In conclusion, the noncalcified plaque area was significantly higher in hemodynamically significant coronary lesions than in nonsignificant lesions. Although an increase in the noncalcified plaque area was significantly associated with a reduced QFR, this association lost significance after adjustment for localized plaque load. **(Am J Cardiol 2023;186:228−235)**

During the past 2 decades, multiple randomized controlled trials have shown that, in terms of clinical outcome, physiology-guided revascularization is superior to revascularization driven by angiographic stenosis severity.[1,2] In addition, angiographic stenosis severity is only modestly associated with the functional consequences of a coronary stenosis.[3] Therefore, interest in the hemodynamic impact, rather than anatomic characteristics, of coronary artery plaques has increased. The "mismatch" between anatomic stenosis severity—assessed by either invasive coronary angiography (ICA) or coronary computed tomography angiography (CTA)—and the hemodynamic impact of a coronary stenosis cannot be fully explained by technical imaging limitations (such as the finite resolution of radiographic imaging). Coronary plaque composition may play an important role in the induction of myocardial ischemia.[4] Although several studies have suggested a pathophysiologic mechanism that underlies the relation between (low-density) noncalcified plaque and inducible myocardial ischemia, conflicting results were found.[5−10] In the present

[a]Departments of Cardiology Leiden University Medical Center, Leiden, The Netherlands; [b]Medis Medical Imaging, Leiden, The Netherlands; [c]Departments of Radiology, Leiden University Medical Center, Leiden, The Netherlands; [d]Heart Center, University of Turku and Turku University Hospital, Turku, Finland; [e]Lambe Institute for Translational Medicine and Curam, National University of Ireland Galway and Saolta University Healthcare Group, University College Hospital Galway, Galway, Ireland; and [f]Division of Cardiology, Icahn School of Medicine at Mount Sinai, New York, New York. Manuscript received July 12, 2022; revised manuscript received and accepted October 3, 2022.

The Department of Cardiology of Leiden University Medical Center received grants from Biotronik (Berlin, Germany), BioVentrix (San Ramon, California), Bayer (Leverkusen, Germany), Medtronic (Minneapolis, Minnesota), Abbott Vascular (Chicago, Illinois), Boston Scientific Corporation (Marlborough, Massachusetts), Edwards Lifesciences (Irvine, California), and GE Healthcare (Chicago, Illinois).

See page 234 for disclosure information.

*Corresponding author: Tel: +31 71 526 2020; fax: +31 71 526 6809.
E-mail address: j.j.bax@lumc.nl (J.J. Bax).

0002-9149/

https://doi.org/10.1016/j.amjcard.2022.10.005

study, our aim was to further clarify the relation between coronary plaque composition and myocardial ischemia in patients with chest pain symptoms. For this purpose, we used intravascular ultrasound virtual histology (IVUS-VH) for the assessment of coronary plaque composition. Quantitative flow ratio (QFR), which is an ICA-based technique used to calculate invasive fractional flow reserve (FFR) without the need for hyperemia induction or for a pressure wire, was used as the reference standard for the evaluation of myocardial ischemia.

Methods

The study population consisted of 103 patients who presented to the outpatient clinic or emergency department of the Leiden University Medical Center with chest pain symptoms. Based on the clinical presentation and/or imaging results, ICA and IVUS-VH were performed for clinical indications to further evaluate the extent and severity of coronary artery disease. Patients with suspected acute or chronic coronary syndrome were evaluated. Clinical data were prospectively entered in the electronic patient file and retrospectively analyzed. The Medical Ethical Committee of the Leiden University Medical Center, The Netherlands, approved this retrospective evaluation of clinically collected data and waived the need for written informed consent.

IVUS-VH was performed during conventional ICA according to standard clinical protocol using a dedicated IVUS console (s5 Imaging System, Volcano Corporation, Rancho Cordova, California). Contraindications for IVUS-VH were (1) severe luminal narrowing, (2) total or subtotal vessel occlusion, and (3) severe vessel tortuosity. After local intracoronary injection of nitroglycerin 200 μg, IVUS-VH was performed with a 20-MHz, 2.9-F phased-array IVUS catheter (Eagle Eye, Volcano Corporation). The IVUS catheter was positioned distally in the coronary artery, and an automatic motorized pullback was performed at a constant speed of 0.5 mm/s until the IVUS catheter reached the guiding catheter. Images were subsequently stored digitally for further offline analysis.

IVUS-VH analysis was performed using a dedicated software package (QCU-CMS 4.59, Medis Medical Imaging, Leiden, The Netherlands and Volcano software, Volcano Corporation, Rancho Cordova, CA). See Figure 1 for the complete workflow of QFR and IVUS-VH analyses. All IVUS-VH examinations were evaluated by 3 experienced observers who were blinded to the clinical data and QFR analysis. Contour detection of the vessel wall, which was defined by the media-adventitia border, and lumen was automatically performed and manually adjusted if needed. Images were analyzed on a per-plaque basis at the site with the smallest cross-sectional luminal area (i.e., the minimal luminal area site). For the analysis, coronary plaques were defined as structures >1 mm^2 that were within and/or adjacent to the coronary artery lumen and could be clearly distinguished from the vessel lumen.[11] Plaque area was calculated as the absolute difference between vessel area and luminal area, whereas localized plaque load was calculated as plaque area / vessel area × 100; both plaque and vessel areas were determined at the minimal luminal area site. Radiofrequency backscatter analysis was used to determine coronary plaque composition. A total of 4 types of plaque composition were differentiated: (1) fibrotic tissue (displayed in dark green on the IVUS-VH images), (2) fibrofatty tissue (displayed in light green), (3) necrotic core tissue (displayed in red), and (4) dense calcium tissue (displayed in white). A noncalcified plaque was defined as a combination of necrotic core and fibrofatty tissue.[12] Plaque composition was reported in both absolute values and percentages of plaque area.

QFR analysis was performed offline using a dedicated software package (QAngio XA 3D/QFR, Medis Medical Imaging, Leiden, The Netherlands). The complete QFR workflow, which is based on 3-dimensional (3D) quantitative coronary angiography and computational fluid dynamics, has been described in detail previously.[13] In short, 2 angiographic views of the coronary artery of interest were selected. Angiographic views were required to be ≥25° apart and to contain minimum vessel overlap and/or foreshortening. Lumen contours were automatically traced on both angiographic views and were manually adjusted if necessary. Subsequently, a 3D model of the coronary artery was reconstructed based on the selected angiographic views. The thrombolysis in myocardial infarction frame count method was used to calculate contrast flow velocity, which was based on the length of the coronary artery segment and the transport time of the injected contrast medium. For this purpose, the angiographic view with the best image quality for contrast flow was used. Finally, hyperemic flow velocity was calculated based on contrast flow velocity, and QFR was computed. In addition, standard quantitative coronary angiography parameters (i.e., diameter of stenosis, lesion length, area of stenosis, and minimal luminal diameter [MLD]) were available for each coronary plaque. Exclusion criteria for QFR analysis were (1) excessive vessel overlap and/or foreshortening, (2) insufficient angiographic image quality, (3) absence of angiographic views ≥25° apart, (4) presence of ostial stenosis, and (5) presence of a coronary stent or bypass graft. Coronary artery plaques with QFR of ≤0.80 were considered abnormal.

QFR was determined distal to all coronary plaques detected with IVUS-VH. When multiple plaques were present per vessel, the most proximal plaque was used for the analysis, and the QFR value was obtained distal to this plaque. To ensure that identical plaques were analyzed with IVUS-VH and QFR, coronary artery segments with plaque were assessed according to the modified 17-segment American Heart Association classification.[14] For this purpose, slice thickness for IVUS-VH and 3D reconstruction for QFR were used to define anatomic markers.

The distribution of continuous variables was determined using histograms and normal quantile-quantile plots. Continuous variables are presented as mean ± SD or as median and interquartile range, as appropriate, and were compared using the independent-sample Student's t test and Mann-Whitney U test, respectively. Categorical variables are presented as number and percentages and were compared using the chi-square test. A univariable logistic regression analysis was performed to assess the association between IVUS-VH plaque characteristics and abnormal QFR. All variables

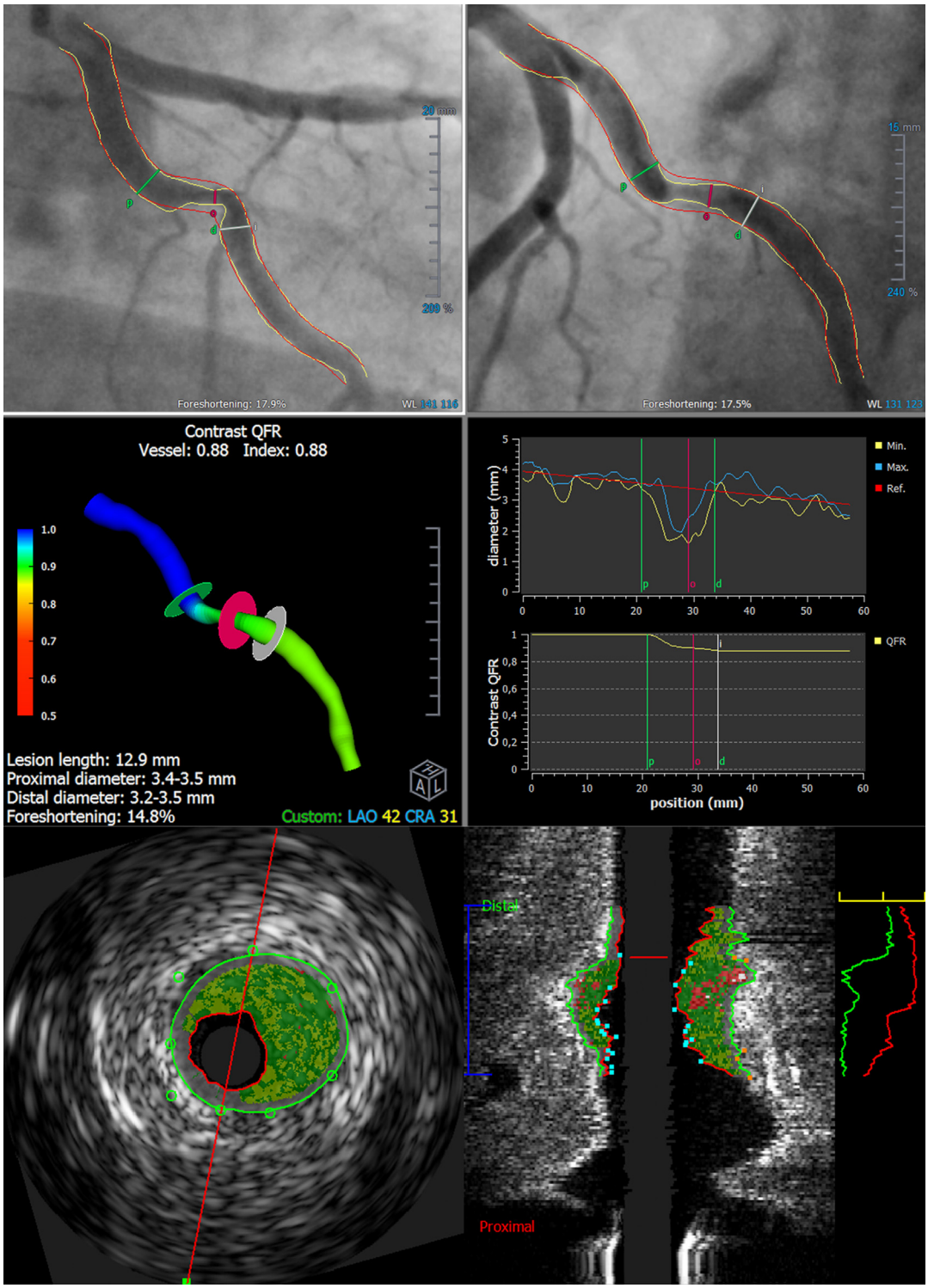

Figure 1. Workflow of QFR and IVUS-VH analyses. Top row (QFR analysis): 2 angiographic views of the coronary artery of interest were selected. Lumen contours were semiautomatically traced on both angiographic views. Middle row (QFR analysis): a 3-dimensional model of the coronary artery was reconstructed based on the selected angiographic views. The thrombolysis in myocardial infarction frame count method was used to calculate contrast flow velocity. Finally, hyperemic flow velocity was calculated based on contrast flow velocity, and QFR was computed. QFR was determined distal to all coronary plaques detected with IVUS-VH. Bottom row (IVUS-VH analysis): contour detection of the vessel wall (defined by the media-adventitia border) and lumen was semiautomatically performed. Images were analyzed on a per-plaque basis at the site with the smallest cross-sectional luminal area. Four types of plaque composition were differentiated: (1) fibrotic tissue (displayed in dark green on the IVUS-VH images), (2) fibrofatty tissue (displayed in light green), (3) necrotic core (displayed in red), and (4) dense calcium tissue (displayed in white). Noncalcified plaque was defined as a combination of necrotic core and fibrofatty tissue.

with p value <0.10 were included in a multivariable analysis. Receiver operating characteristic curves were constructed for the discrimination between normal and abnormal QFR using IVUS-VH plaque characteristics. The receiver operating characteristic area under the curve (AUC) was compared between IVUS-VH plaque characteristics, using the method of DeLong et al.[15] All statistical analyses were performed with SPSS software (IBM Corp Released 2015; IBM SPSS Statistics for Windows, Version 25.0; Armonk, New York: IBM Corp) and MedCalc 18.2.1 for Windows (MedCalc Software, Ostend, Belgium). Statistical tests were considered significant if the 2-sided p <0.05.

Results

A total of 103 patients (mean age 58 ± 10 years, 67% male) who underwent ICA and subsequent IVUS-VH were included. Overall, 68 patients (66%) and 35 patients (34%) presented with suspected acute and chronic coronary syndrome, respectively. A complete overview of the patient characteristics is displayed in Table 1.

In total, 171 coronary plaques were analyzed. Twenty-two plaques (13%) were excluded from QFR analysis because of foreshortening (n = 4), presence of a stent (n = 5), absence of coronary plaques on ICA (n = 3), poor image quality (n = 1), distal location of the coronary plaque (n = 3), diffuse disease (n = 2), ostial lesion (n = 2), coronary occlusion (n = 1) or vessel overlap (n = 1). Of the remaining 149 plaques, 68 (46%) were located in the left anterior descending coronary artery, 28 (19%) in the left circumflex coronary artery, 38 (26%) in the right coronary artery, 1 (1%) in the left main coronary artery, and 14 (9%) in a coronary side branch (Table 2). According to QFR, 21 plaques (14%) were hemodynamically significant and 128 (86%) were nonsignificant. A complete overview of the plaque characteristics is displayed in Table 2.

Mean plaque area and plaque load, as determined with IVUS-VH, were 8.2 ± 7.7 mm^2 and 54 ± 12%, respectively. Coronary plaques were predominantly composed of fibrotic tissue (57.5 ± 12.2%), followed by fibrofatty tissue (18.4 ± 10.9%), necrotic core (15.4 ± 9.0%), and dense calcium tissue (8.6 ± 11.3%). Plaques with abnormal QFR had significantly larger plaque area (10.8 ± 4.6 mm^2 vs 7.8 ± 2.8 mm^2, p = 0.008) and plaque load (64.8 ± 13.0% vs 52.7 ± 11.3%, p <0.001) compared with plaques with preserved QFR (Table 3). Moreover, fibrotic (p = 0.001), fibrofatty (p = 0.001) and necrotic core (p = 0.006) areas were significantly larger in plaques with abnormal QFR, whereas no significant difference was found for dense calcium area (p = 0.21). Although the percentages of fibrotic tissue (p = 0.31), fibrofatty tissue (p = 0.12), necrotic core (p = 0.56) and dense calcium tissue (p = 0.76) were not significantly different between plaques with abnormal and normal QFR, the percentage of noncalcified tissue was significantly higher in plaques with abnormal QFR (38.2 ± 6.5% vs 33.1 ± 9.0%, p = 0.014). In the subgroup of plaques in the lowest MLD quartile, plaques with abnormal QFR had a significantly larger noncalcified plaque load compared with plaques with preserved QFR (38.5 ± 7.3% vs 30.8 ± 5.7%, p = 0.001) (Figure 2, Table 4). However, compositional plaque load did not significantly differ between plaques with abnormal and normal QFR in the remaining MLD quartile subgroups.

The AUC for discrimination between abnormal and normal QFR was significantly higher for plaque load than for the percentage of dense calcium (difference between AUCs 0.25, p = 0.012) or fibrotic (difference between AUCs 0.17, p = 0.033) tissue but not for the percentage of noncalcified tissue (difference between AUCs 0.08, p = 0.31) (Figure 3). By univariable analysis, both plaque load (odds ratio [OR] per 1% increase 1.081, p <0.001) and the percentage of noncalcified tissue (OR per 1% increase 1.070, p = 0.020) were significantly associated with abnormal QFR (Table 5). However, by multivariable analysis, only plaque load

Table 1
Baseline patient characteristics

	Total (n = 103)
Age (years)	58±10
Male	69 (67%)
Cardiovascular risk factors	
Hypertension	61 (59%)
Hypercholesterolemia	52 (51%)
Diabetes	28 (27%)
Obesity (BMI ≥30 kg/m^2)	22 (21%)
Family history of CAD	50 (49%)
Current smoker	37 (36%)
Prior MI	21 (20%)
Prior PCI	25 (24%)
Medication use	
Beta blockers	54 (52%)
ACE inhibitors/ARBs	53 (52%)
Aspirin	53 (52%)
Statins	64 (62%)
Presentation with suspected ACS	68 (66%)

Values are mean ± SD or n (%).

ACE = angiotensin-converting enzyme; ACS = acute coronary syndrome; ARB = angiotensin II receptor blocker; BMI = body mass index; CAD = coronary artery disease; MI = myocardial infarction; PCI = percutaneous coronary intervention.

Table 2
Baseline plaque characteristics

	Total (n = 149)
Analyzed vessels	
Left anterior descending coronary artery	68 (46%)
Left circumflex coronary artery	28 (19%)
Right coronary artery	38 (26%)
Left main coronary artery	1 (1%)
Coronary side branch	
First diagonal branch	1 (1%)
Second diagonal branch	2 (1%)
Intermediate or anterolateral branch	4 (3%)
Obtuse marginal branch	7 (5%)
Lesion length (mm)	16 (11−23)
Stenosis diameter (%)	38±14
Stenosis area (%)	51±18
Minimal lumen diameter (mm)	1.9±0.6
QFR	0.95 (0.87−0.99)

Values are mean ± SD, median (interquartile range), or n (%).

QFR = quantitative flow ratio.

Table 3
IVUS-VH plaque characteristics, according to QFR

IVUS-VH parameter	QFR ≤0.80 (n = 21)	QFR >0.80 (n = 128)	P Value
Anatomic plaque characteristics			
Lumen area (mm^2)	5.6 (3.4−7.0)	7.0 (4.4−8.7)	**0.031**
Vessel area (mm^2)	16.4±5.3	14.9±5.1	0.23
Plaque area (mm^2)	10.8±4.6	7.8±2.8	**0.008**
Plaque load (%)	64.8±13.0	52.7±11.3	**<0.001**
Compositional plaque characteristics			
Fibrotic area (mm^2)	3.90 (3.00−4.81)	2.33 (1.68−3.52)	**0.001**
Fibrofatty area (mm^2)	1.30 (0.73−2.24)	0.67 (0.31−1.27)	**0.001**
Necrotic core area (mm^2)	1.10 (0.56−1.98)	0.59 (0.30−1.04)	**0.006**
Dense calcium area (mm^2)	0.33 (0.14−0.83)	0.24 (0.10−0.46)	0.21
Noncalcified area (mm^2) *	2.20 (0.54−4.16)	1.42 (0.81−2.03)	**<0.001**
Fibrotic (%)	55.0±9.7	57.9±12.5	0.31
Fibrofatty (%)	18.0 (13.5−27.4)	16.5 (10.5−24.5)	0.12
Necrotic core (%)	16.5±8.7	15.3±9.0	0.56
Dense calcium (%)	4.2 (2.7−11.2)	6.4 (2.3−10.5)	0.76
Noncalcified (%)*	38.2±6.5	33.1±9.0	**0.014**

Values are mean ± SD or median (interquartile range).
* Noncalcified was defined as a combination of fibrofatty and necrotic core plaque.IVUS-VH = intravascular ultrasound virtual histology; QFR = quantitative flow ratio.

remained significantly associated with abnormal QFR (OR per 1% increase 1.072, p <0.001).

Discussion

In this study, we investigated the relation between coronary plaque composition and myocardial ischemia in patients with chest pain symptoms. We showed that the noncalcified plaque area was significantly higher in hemodynamically significant coronary lesions (defined by a QFR ≤0.80) than in nonsignificant lesions (defined by a QFR >0.80). Moreover, an increase in localized plaque load and noncalcified plaque area, but not in fibrotic or dense calcium plaque area, was significantly associated with abnormal QFR. However, by multivariable analysis, only plaque load remained independently associated with abnormal QFR.

In recent years, multiple studies have analyzed the relation between plaque composition and the hemodynamic significance of coronary lesions. In these studies, coronary plaque composition was assessed by either quantitative coronary CTA or IVUS-VH, whereas the presence of myocardial ischemia was determined from positron emission tomography perfusion imaging or invasive FFR. Driessen et al[6] evaluated the effects of plaque load and composition on myocardial blood flow and invasive FFR in a post hoc substudy from the PACIFIC trial. The substudy included 208 patients with suspected coronary artery disease who prospectively underwent coronary CTA, positron emission tomography perfusion imaging, and invasive FFR measurements. It was demonstrated that noncalcified plaque and positive remodeling were significantly associated with reduced myocardial blood flow and invasive FFR, independent of luminal stenosis. Also, Imai et al[7] investigated the relation between coronary plaque characteristics and invasive FFR. The study analyzed nonobstructive lesions, which were defined as <50% stenosis by quantitative coronary angiography, in 108 patients who underwent coronary CTA and ICA. Subsequently, coronary CTA characteristics of nonobstructive lesions with FFR ≤0.80 (i.e., anatomy-physiology mismatch) were compared with those of nonobstructive lesions with FFR >0.80 (i.e., anatomy-physiology match). In the absence of anatomically significant stenosis, the presence of positive remodeling, larger plaque load, and low-attenuation plaque (an indicator of necrotic core on CTA) was associated with abnormal FFR. In addition, Gaur et al[8] performed a post hoc substudy in 484 vessels in 254 patients from the NXT trial to assess the association between coronary stenosis, plaque composition, coronary CTA-derived FFR, and invasive FFR. Interestingly, low-density noncalcified plaque was significantly associated with myocardial ischemia assessed by invasive FFR, independent of total plaque volume. Waksman et al[9] evaluated IVUS-VH parameters in relation to invasive FFR in 350 patients with 367 intermediate coronary lesions (defined as 40% to 80% stenosis by ICA).[9] In contrast to results from most coronary CTA studies, plaque composition by IVUS-VH showed no correlation with invasive FFR for the detection of myocardial ischemia. The relation between IVUS-VH parameters and invasive FFR was also assessed by Brown et al[10] in 92 lesions in 89 patients with stable angina. The authors found no relation between IVUS-VH-defined plaque composition and invasive FFR.

FFR is the ratio of the hyperemic myocardial flow in a stenotic territory to the normal hyperemic myocardial flow (i.e., in the absence of coronary stenoses).[16] For FFR measurement, it is essential to induce maximal vasodilation of the epicardial coronary artery (e.g., by nitroglycerin administration) and the microvasculature (e.g., by adenosine administration). Only under these circumstances can FFR be correctly calculated from the ratio of distal coronary pressure to aortic pressure.

Although several studies have shown a relation between coronary plaque composition and invasive FFR, the underlying pathophysiologic link remains unclear. It has been thought that the presence of a necrotic core in noncalcified

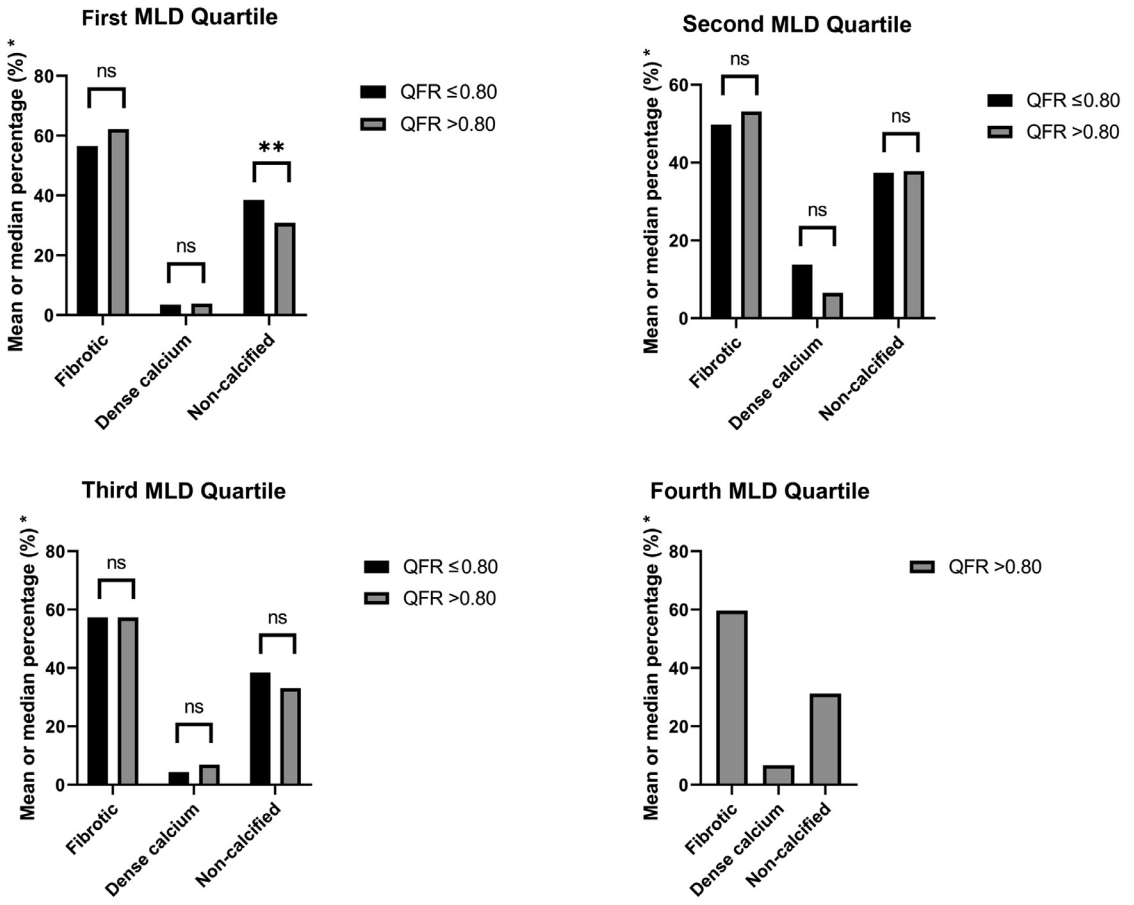

Figure 2. IVUS-VH plaque composition, according to MLD quartiles and QFR. In the subgroup of plaques in the lowest MLD quartile, plaques with abnormal QFR had a significantly larger noncalcified plaque load compared with plaques with preserved QFR (38.5 ± 7.3% vs 30.8 ± 5.7%, p = 0.001). However, compositional plaque load did not significantly differ between plaques with abnormal and normal QFR in the remaining MLD quartile subgroups.

Table 4
IVUS-VH plaque composition, according to MLD quartiles and QFR

	QFR ≤0.80	QFR >0.80	P Value
MLD quartile			
1	14 (40%)	21 (60%)	
Fibrotic (%)	56.5±9.6	62.2±8.8	0.082
Dense calcium (%)	3.5 (1.5−8.1)	3.8 (1.5−10.1)	0.64
Noncalcified (%)	38.5±7.3	30.8±5.7	**0.001**
2	5 (15%)	28 (85%)	
Fibrotic (%)	49.8±10.0	53.1±15.8	0.66
Dense calcium (%)	13.8 (7.6−17.5)	6.5 (2.0−8.0)	0.097
Noncalcified (%)	37.4±3.8	37.8±11.0	0.94
3	2 (5%)	37 (95%)	
Fibrotic (%)	57.3±9.4	57.3±12.4	1.00
Dense calcium (%)	4.3 (4.0−4.3)	6.9 (2.9−12.1)	0.41
Noncalcified (%)	38.4±9.0	33.1±8.0	0.38
4	0	42 (100%)	
Fibrotic (%)	N/A	59.6±11.0	N/A
Dense calcium (%)	N/A	6.6 (2.2−10.5)	N/A
Noncalcified (%)	N/A	31.2±8.8	N/A

IVUS-VH = intravascular ultrasound virtual histology; MLD = minimal lumen diameter; QFR = quantitative flow ratio.

plaque leads to local endothelial dysfunction, oxidative stress, and inflammation.[4,17,18] This may suggest that noncalcified plaques with necrotic core do not allow adequate vasodilation of the epicardial coronary artery during nitroglycerin administration. As a consequence, vasodilation of the stenotic noncalcified coronary segment may be reduced relative to vasodilation of the remainder of the vessel, resulting in an increased pressure decrease and lower FFR value.

In our study, QFR was used as the reference standard for myocardial ischemia and was compared with coronary plaque composition defined by IVUS-VH. QFR is a relatively novel technique to calculate FFR without hyperemia induction or the need for a pressure wire.[19] QFR calculation is based on coronary tree reconstruction by 3D quantitative coronary angiography and computational fluid dynamics. As opposed to invasive FFR, QFR computation is derived from angiographic views performed under baseline conditions (i.e., without hyperemia induction). Therefore, coronary flow modification induced by hyperemic agents, which leads to vasodilation of the epicardial coronary artery and microvasculature, has been omitted from QFR calculation. Instead, the hyperemic flow velocity is modeled under

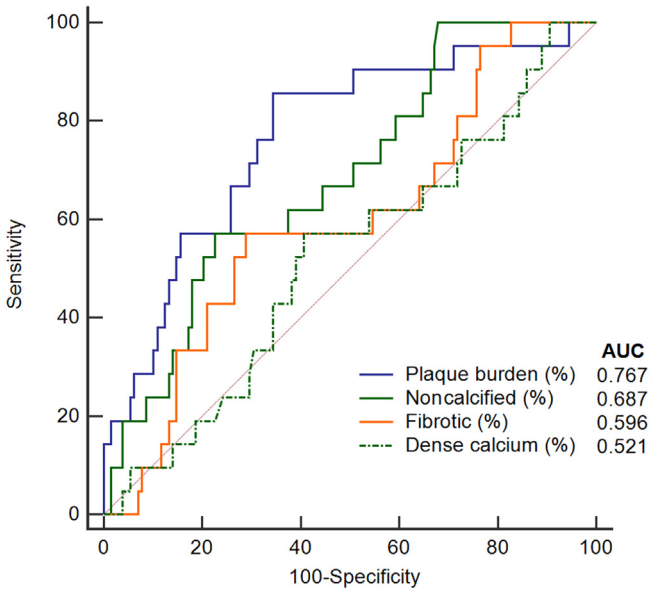

Figure 3. Receiver operating characteristic curve analysis for discrimination between abnormal (≤0.80) and normal (>0.80) QFR using IVUS-VH plaque characteristics. The AUC was significantly higher for plaque load than for the percentage of dense calcium (difference between AUCs 0.25, p = 0.012) or fibrotic (difference between AUCs 0.17, p = 0.033) tissue. However, no significant difference was found between the AUCs for plaque load and the percentage of noncalcified tissue (difference between AUCs 0.08, p = 0.31).

baseline conditions using the contrast flow velocity and is therefore based on the assumption that the hyperemic response to nitroglycerin and adenosine is predictable.[20] In this study, we found a significant relation between the noncalcified plaque area and QFR. However, this relation was not significant after adjustment for localized plaque load in multivariable analysis. These findings are in accordance with a recent substudy of the PACIFIC trial, which showed an independent association of CT-derived adverse plaque characteristics with hyperemic FFR measurements but not with nonhyperemic instantaneous wave-free ratio.[21] This may be explained by the omission of coronary plaque composition—and its potential effect on local coronary vasodilation—from QFR and instantaneous wave-free ratio computation.

Our study has several limitations. First, coronary angiography images were retrospectively evaluated for QFR analysis. Therefore, 13% of coronary plaques were excluded from our analysis because of suboptimal image quality. Second, IVUS-VH analysis was not performed for the entire coronary plaque or vessel, but only for the plaque site with the smallest cross-sectional luminal area. Third, when multiple plaques per vessel were present, only the most proximal plaque was used for the analysis, and the QFR value was obtained distal to this plaque. The potential effects of distal coronary plaques on coronary hemodynamics and the QFR value were thereby ignored. Fourth, QFR analysis was performed only under baseline conditions (i.e., without hyperemia induction). Therefore, we were unable to confirm our hypothesis that noncalcified plaques with necrotic core do not allow adequate vasodilation under hyperemic conditions; the noncalcified plaque area showed no independent association with QFR. Importantly, the proposed mechanism that noncalcified plaques induce a higher risk of myocardial ischemia should be regarded as hypothesis-generating.

In conclusion, we showed that the noncalcified plaque area was significantly higher in hemodynamically significant coronary lesions (defined by a QFR ≤0.80) than in nonsignificant lesions (defined by a QFR >0.80). Although an increase in the noncalcified plaque area was significantly associated with an abnormal QFR, this association lost significance after adjustment for localized plaque load. Future research should focus on the underlying pathophysiologic mechanisms of coronary plaque composition that affect myocardial perfusion and its potential applicability in clinical practice.

Table 5
Logistic regression analysis for the detection of abnormal QFR (≤0.80)

	Univariable		Multivariable	
IVUS-VH parameter	OR	p Value	OR	p Value
Plaque load (per 1% increase)	1.081	**<0.001**	1.072	**0.001**
Fibrotic (per 1% increase)	1.030	0.14		
Dense calcium (per 1% increase)	0.977	0.42		
Noncalcified (per 1% increase)*	1.070	**0.020**	1.035	0.28

* Noncalcified was defined as a combination of fibrofatty and necrotic core plaque.

IVUS-VH = intravascular ultrasound virtual histology; OR = odds ratio; QFR = quantitative flow ratio.

Disclosures

Dr. Bax received speaker fees from Abbott Vascular. Dr. Wijns is cofounder of Argonauts, is medical advisor to Rede Optimus Research, and received institutional research grants and honoraria from MicroPort. The remaining authors have no conflicts of interest to declare.

1. Tonino PAL, De Bruyne B, Pijls NHJ, Siebert U, Ikeno F, van' t Veer M, Klauss V, Manoharan G, Engstrøm T, Oldroyd KG, Ver Lee PN, MacCarthy PA, Fearon WF, FAME Study Investigators. Fractional flow reserve versus angiography for guiding percutaneous coronary intervention. *N Engl J Med* 2009;360:213–224.
2. van Nunen LX, Zimmermann FM, Tonino PAL, Barbato E, Baumbach A, Engstrøm T, Klauss V, MacCarthy PA, Manoharan G, Oldroyd KG, Ver Lee PN, van't Veer M, Fearon WF, De Bruyne B, Pijls NHJ, FAME Study Investigators. Fractional flow reserve versus angiography for guidance of PCI in patients with multivessel coronary artery disease (FAME): 5-year follow-up of a randomised controlled trial. *Lancet* 2015;386:1853–1860.
3. Tonino PAL, Fearon WF, De Bruyne B, Oldroyd KG, Leesar MA, Ver Lee PN, MacCarthy PA, van't Veer M, Pijls NHJ. Angiographic versus functional severity of coronary artery stenoses in the FAME study fractional flow reserve versus angiography in multivessel evaluation. *J Am Coll Cardiol* 2010;55:2816–2821.
4. Ahmadi A, Stone GW, Leipsic J, Serruys PW, Shaw L, Hecht H, Wong G, Nørgaard BL, O'Gara PT, Chandrashekhar Y, Narula J. Association of coronary stenosis and plaque morphology with fractional flow reserve and outcomes. *JAMA Cardiol* 2016;1:350–357.
5. Xaplanteris P, de Hemptinne Q. The relationship between plaque morphology and its hemodynamic significance. American College of Cardiology. Available at: *https://www.acc.org/latest-in-cardiology/articles/2018/10/30/09/08/the-relationship-between-plaque-morphology-and-its-hemodynamic-significance?report=reader*. Accessed October 1, 2022.

6. Driessen RS, Stuijfzand WJ, Raijmakers PG, Danad I, Min JK, Leipsic JA, Ahmadi A, Narula J, van de Ven PM, Huisman MC, Lammertsma AA, van Rossum AC, van Royen N, Knaapen P. Effect of plaque burden and morphology on myocardial blood flow and fractional flow reserve. *J Am Coll Cardiol* 2018;71:499–509.
7. Imai S, Kondo T, Stone GW, Kawase Y, Ahmadi AA, Narula J, Matsuo H. Abnormal fractional flow reserve in nonobstructive coronary artery disease. *Circ Cardiovasc Interv* 2019;12:e006961.
8. Gaur S, Øvrehus KA, Dey D, Leipsic J, Bøtker HE, Jensen JM, Narula J, Ahmadi A, Achenbach S, Ko BS, Christiansen EH, Kaltoft AK, Berman DS, Bezerra H, Lassen JF, Nørgaard BL. Coronary plaque quantification and fractional flow reserve by coronary computed tomography angiography identify ischaemia-causing lesions. *Eur Heart J* 2016;37:1220–1227.
9. Waksman R, Legutko J, Singh J, Orlando Q, Marso S, Schloss T, Tugaoen J, DeVries J, Palmer N, Haude M, Swymelar S, Torguson R. FIRST: Fractional Flow Reserve and Intravascular Ultrasound RelationShip STudy. *J Am Coll Cardiol* 2013;61:917–923.
10. Brown AJ, Giblett JP, Bennett MR, West NEJ, Hoole SP. Anatomical plaque and vessel characteristics are associated with hemodynamic indices including fractional flow reserve and coronary flow reserve: a prospective exploratory intravascular ultrasound analysis. *Int J Cardiol* 2017;248:92–96.
11. Leber AW, Knez A, Becker A, Becker C, von Ziegler F, Nikolaou K, Rist C, Reiser M, White C, Steinbeck G, Boekstegers P. Accuracy of multidetector spiral computed tomography in identifying and differentiating the composition of coronary atherosclerotic plaques: a comparative study with intracoronary ultrasound. *J Am Coll Cardiol* 2004;43:1241–1247.
12. Voros S, Rinehart S, Qian Z, Vazquez G, Anderson H, Murrieta L, Wilmer C, Carlson H, Taylor K, Ballard W, Karmpaliotis D, Kalynych A, Brown C III. Prospective validation of standardized, 3-dimensional, quantitative coronary computed tomographic plaque measurements using radiofrequency backscatter intravascular ultrasound as reference standard in intermediate coronary arterial lesions: results from the ATLANTA (Assessment of Tissue characteristics, Lesion morphology, and hemodynamics by angiography with fractional flow reserve, intravascular ultrasound and virtual histology, and Noninvasive computed Tomography in Atherosclerotic plaques) I study. *JACC Cardiovasc Interv* 2011;4:198–208.
13. Smit JM, Koning G, van Rosendael AR, Dibbets-Schneider P, Mertens BJ, Jukema JW, Delgado V, Reiber JHC, Bax JJ, Scholte AJ. Relationship between coronary contrast-flow quantitative flow ratio and myocardial ischemia assessed by SPECT MPI. *Eur J Nucl Med Mol Imaging* 2017;44:1888–1896.
14. Austen WG, Edwards JE, Frye RL, Gensini GG, Gott VL, Griffith LS, McGoon DC, Murphy ML, Roe BB. A reporting system on patients evaluated for coronary artery disease. Report of the Ad Hoc Committee for Grading of Coronary Artery Disease, Council on Cardiovascular Surgery, American Heart Association. *Circulation* 1975;51(suppl):5–40.
15. DeLong ER, DeLong DM, Clarke-Pearson DL. Comparing the areas under two or more correlated receiver operating characteristic curves: a nonparametric approach. *Biometrics* 1988;44:837–845.
16. De Bruyne B, Sarma J. Fractional flow reserve: a review: invasive imaging. *Heart* 2008;94:949–959.
17. Lavi S, McConnell JP, Rihal CS, Prasad A, Mathew V, Lerman LO, Lerman A. Local production of lipoprotein-associated phospholipase A2 and lysophosphatidylcholine in the coronary circulation: association with early coronary atherosclerosis and endothelial dysfunction in humans. *Circulation* 2007;115:2715–2721.
18. Lavi S, Yang EH, Prasad A, Mathew V, Barsness GW, Rihal CS, Lerman LO, Lerman A. The interaction between coronary endothelial dysfunction, local oxidative stress, and endogenous nitric oxide in humans. *Hypertension* 2008;51:127–133.
19. Smit JM, El Mahdiui M, van Rosendael AR, Jukema JW, Koning G, Reiber JHC, Bax JJ, Scholte AJ. Comparison of diagnostic performance of quantitative flow ratio in patients with versus without diabetes mellitus. *Am J Cardiol* 2019;123:1722–1728.
20. Mejía-Rentería H, Lee JM, Lauri F, van der Hoeven NW, de Waard GA, Macaya F, Pérez-Vizcayno MJ, Gonzalo N, Jiménez-Quevedo P, Nombela-Franco L, Salinas P, Núñez-Gil I, Del Trigo M, Goto S, Lee HJ, Liontou C, Fernández-Ortiz A, Macaya C, van Royen N, Koo BK, Escaned J. Influence of microcirculatory dysfunction on angiography-based functional assessment of coronary stenoses. *JACC Cardiovasc Interv* 2018;11:741–753.
21. Driessen RS, de Waard GA, Stuijfzand WJ, Raijmakers PG, Danad I, Bom MJ, Min JK, Leipsic JA, Ahmadi A, van de Ven PM, Knuuti J, van Rossum AC, Davies JE, van Royen N, Narula J, Knaapen P. Adverse plaque characteristics relate more strongly with hyperemic fractional flow reserve and instantaneous wave-free ratio than with resting instantaneous wave-free ratio. *JACC Cardiovasc Imaging* 2020;13:746–756.